ON THE DISTRIBUTION OF AMBIGUITY LEVELS IN MIMO RADAR

M. A. Haleem and A. Haimovich
Department of Electrical and Computer Engineering,
New Jersey Institute of Technology, Newark, NJ 07102.
{haleem, alexander.m.haimovich}@njit.edu

***Abstract*—The statistical behavior of sidelobe-ambiguity arising in location estimation in distributed coherent MIMO radar is studied in this paper. A model is developed for analyzing the statistics of the localization metric under random sensor locations. Closed form expressions are obtained for the mean and variance of the localization metric. It is shown that the mean is independent of the number of sensors and its sidelobes decrease with the squared distance from the coherence point of the MIMO array. With M transmit sensors and N receive sensors, the variance behaves as $1/MN$ for locations beyond the vicinity of the target being observed. When all N sensors function as transceivers, the variance approaches $2/N^2$. Except in the vicinity of the target, the side lobe levels have equal distribution at every location. The study is extended to derive the statistics of the peak sidelobe level and a simple expression is obtained relating the required number of sensors for a tolerated level of peak sidelobes and a desired confidence level.**

***Index Terms*—MIMO radar, Ambiguity, radiation pattern.**

I. INTRODUCTION

MIMO radars with distributed sensors have emerged as a technology with great potential for surveillance, high accuracy target localization, and imaging. When a large, extended target (or group of small targets) presents to distributed radar sensors different radar cross section (RCS) aspects, non-coherent combination of these returns enhances performance for high probability of detection cases [1],[2]. Alternatively, when the target is too small or too far, and the returns are coherent across the MIMO radar sensors, coherent processing can greatly enhance the target localization ability leading to resolutions limited by the carrier frequency rather than the signal bandwidth [3],[4]. However, the high resolution capability comes at the cost of numerous and high sidelobes, i.e., ambiguities in the localization metric. The sidelobes are rooted in the severe undersampling of the signals returned from the target. A related effect is the presence of grating lobes in linear arrays with thinned, but uniformly spaced, elements. In the 1970's and 1980's, Steinberg and collaborators at the University of Pennsylvania studied and built a thinned, large, linear array system with randomly placed elements and have demonstrated its superior resolution abilities for direction finding [7],[8]. In context, coherent MIMO radar with distributed sensors may be viewed as an extension of these early large, linear arrays to two dimensional arrays with multiple transmitting and receiving sensors.

The problem addressed in this paper is concerned with the ambiguity due to sidelobe levels arising in the localization metric. While the sensors and processing of the system is tuned to a resolution cell, a target at a different location may be detected through a sidelobe leading to ambiguities in localization. Sensors are spaced by hundreds of wavelengths and are randomly placed with respect to a surveillance area. Resolution cells in the surveillance area are tested for the presence of targets. Relevant to this effort is the literature on linear, random arrays. In [5] and [6], Lo has established the mathematical framework for studying the statistical behavior of random, linear arrays. Later, Steinberg and others extended these initial studies to examine the effect of different parameters such as number of elements, wavelength, element size, beam steering angle, and signal bandwidth (for example [7],[8]). These studies are basically concerned with angle of arrival estimation of a signal received from a target and hence assume *far-field* radiation patterns. Our present problem, namely that of distributed MIMO radar, is concerned with localization (range and angle) in two dimensional space, and the analysis assumes sensors, each at a different angle with respect to the surveillance area, i.e., the targets are in the *near-field* with respect to the MIMO radar system. In the near field, the phase of the signal bouncing off the target is a function not only of the angle of arrival, but also of the sensor-target range. When processed jointly, distributed sensors form large, virtual apertures resulting in *very high resolution* capabilities.

In the sections to follow, we introduce the problem model in Section II. The statistics of the localization metric are analyzed in Section III. Closed form expressions for mean and variance of the metric as functions of spatial coordinates are presented in this section. The sidelobe at any given location is modeled using a Gaussian distribution, thus allowing the computation of different percentile probabilities of the sidelobe levels within the surveillance area (visible region). The distribution of peak sidelobe level in the visible region is studied next. The paper concludes with Section IV.

II. DISTRIBUTED COHERENT MIMO RADAR - ANALYTICAL MODEL

We seek to study the localization properties of MIMO radar with distributed sensors and coherent processing. In particular, we are interested in determining the sidelobe properties of the localization metric. Coherent processing among the sensors implies a global phase reference. To further elaborate, consider the scenario depicted in Fig. 1. For simplicity, we assume that the target has to be located in a plane rather than a volume. A signal waveform is transmitted from sensor k at location P defined by the polar coordinates (ρ_k, θ_k), where θ_k is measured with respect to an arbitrary horizontal axis.

The coordinate system has the origin at O and its orientation is arbitrary. Sensors are placed randomly in a sector extending between $-\theta_{\max}$ and $\theta_{\max}$. In MIMO radar, sensors may transmit different signals or the same signal. In the former case, each receiver consists of matched filters to all the transmitted signals. The surveillance space is illuminated isotropically, if each sensor transmits isotropically. The localization metric is formed by post-processing at the receiver. Alternatively, all sensors may transmit the same waveform. With suitable phase shifts at each sensor, the energy may be cohered at the desired observation point O. In this case, the processing is divided between the transmitter (phase shifts to cohere the energy) and the receiver (a set of phase shifts applied to the received signals to cohere the energy at the observation point). For simplicity of presentation, we adopt the point of view of a single waveform.

Given a MIMO radar system with M transmit and N receive sensors cohered at O, we are asking what is the response to a point target at location R, specified by its polar coordinates (ρ, α). When a target is found at O, complete coherency is achieved for all the transmit/receive sensor pairs and the resultant signal is maximized. When the target is at R, the phase compensation is not perfect. As the point of interest R is varied over the two dimensional surveillance area, the resultant signal forms a pattern with peaks and valleys. In

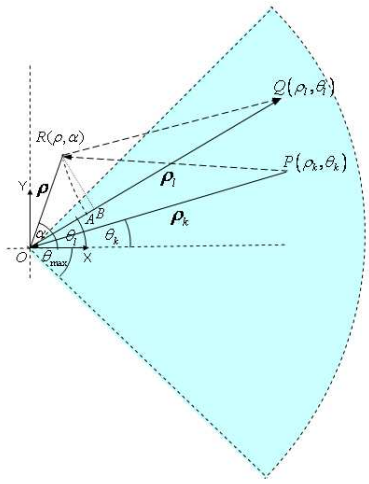

Fig. 1. Analytical model for sidelobes of the localization metric.

this work, we focus on the effect of phase, so the transmitted waveform is assumed narrowband in the sense that changes in the envelope of the received signal over the surveillance area are negligible. This is a conservative assumption with respect to the level of the sidelobes, since the autocorrelation function of the envelope will serve as an upper bound to any sidelobes. It can be shown that under these conditions and for an $M \times N$ system, the localization metric under coherent combining expressed as a function of an index of points in the surveillance area can be written [3]

$$A(\xi) = \frac{1}{MN} \sum_{k=1}^{M} \sum_{l=1}^{N} e^{-j2\pi f_0 \tau_{k\xi l}}, \tag{1}$$

where f_0 is the carrier frequency. The metric is normalized such that its peak value is 1. With reference to Fig. 1, $\tau_{k\xi l}$ is the differential between the time delays of paths $P-R-Q$ and $P-O-Q$. Considering the paths from the coherence point O and from the sidelobe point R to the receive sensor l, $\tau_{\xi l} = \frac{-OA}{c}$, where c is the speed of light. We have $OA = OQ - RQ = \rho_l \left[1 - \sqrt{1 - \left(\frac{2\rho}{\rho_l}\cos(\alpha - \theta_l) - \frac{\rho^2}{\rho_l^2}\right)}\right]$, where the polar coordinates of R and Q are respectively, (ρ, α) and (ρ_l, θ_l). When $\rho << \rho_l$, $OA \approx \rho\cos(\alpha - \theta_l)$. It is seen that under this model, the differential delay is dependent only on the bearing angle of the sensor l with respect to the origin O.

It is further assumed that while the angles θ_k and θ_l formed by different sensors are *distinct*, the surveillance area of interest is such that all targets in the area are viewed by a sensor at the *same* angle. For example, sensor k, views all targets at angle θ_k. This implies that the separation between sensors is of the scale of the distance of the sensors from the surveillance area, but that the surveillance area is much smaller than this scale.

For a given location ξ, $A(\xi)$ is a random variable function of the random sensor locations. As the location index ξ is varied, $A(\xi)$ becomes a stochastic process. In the following section, we study the statistics of this process.

III. Statistics of the Localization Metric

The statistical properties of the localization metric are discussed in this section. Two different sensor configurations are considered. In the first case, there are M transmit sensors which are distinct from N receive sensors. Thus, the total number of sensors in this case is $M+N$. In the second case, there are N sensors, all operating as transceivers. In each case, the statistics are derived considering two different distributions for the sensor locations. One distribution considered is a uniform distribution for the bearing angles of the sensors θ_k, θ_l. The angles θ_k, θ_l are assumed independent and identically distributed (iid) for $k = 1, \cdots, M$ and $l = 1, \cdots, N$. With the other distribution, the random variables $u_k = \cos(\alpha - \theta_k)$ and $v_l = \cos(\alpha - \theta_l)$ are iid uniform. The latter model lends itself to analysis, and numerical results show that there is not much difference between the models.

A. Mean and Variance

The mean and variance of the localization metric are derived for distinct transmit and receive sensors and for transceivers. Properties are illustrated by numerical examples.

1) Distinct transmitters and receivers: Using quantities introduced previously, and assuming that the distance ρ with respect to the coherence point of a point in the sidelobes is normalized to the wavelength, the localization metric (1) can be expressed at some point (ρ, α) as

$$A(\rho, \alpha) = \frac{1}{MN} \sum_{k=1}^{M} \sum_{l=1}^{N} e^{j2\pi\rho(u_k + v_l)}. \tag{2}$$

With M transmitters and N receivers, the mean $\phi(\rho, \alpha)$ of the localization metric is found by taking the expectation

$E[A(\rho,\alpha)]$ over u_k and v_l as follows.

$$\phi(\rho,\alpha) = E\left[\frac{1}{MN}\sum_{k=1}^{M}\sum_{l=1}^{N} e^{j2\pi\rho(u_k+v_l)}\right] \tag{3}$$

The expectation and summation can be interchanged, then the expectations of the terms in the summation become identical for all pairs of indices k and l. Thus, in the sequel, the random variables are written as u and v without the indices. We have a sum of MN identical terms leading to

$$\begin{aligned}\phi(\rho,\alpha) &= E\left[e^{j2\pi\rho(u+v)}\right] \\ &= E\left[e^{j2\pi\rho u}\right]E\left[e^{j2\pi\rho v}\right]. \end{aligned} \tag{4}$$

Last step in (4) follows from the independence between u and v. Reasonably assuming identical distribution for u and v, we obtain

$$\phi(\rho,\alpha) = \psi^2(\rho,\alpha), \tag{5}$$

where $\psi(\rho,\alpha) = E\left[e^{j2\pi\rho u}\right]$ is the *characteristic function* of u which can be computed for a known pdf of u, $f(u)$. As mentioned earlier, we consider two different pdf's governing the location of the sensors. The expectation computed here is the mean of the localization metric for a continuous aperture with an excitation function given by $f(u)$. The variance of the localization metric is given by,

$$\begin{aligned}\sigma^2 &= E\left[\left(A(\rho,\alpha)-\phi(\rho,\alpha)\right)\left(A(\rho,\alpha)-\phi(\rho,\alpha)\right)^*\right] \\ &= E\left[\left|A(\rho,\alpha)-\phi(\rho,\alpha)\right|^2\right]. \end{aligned} \tag{6}$$

Substitution from (2) and (5) leads to

$$\begin{aligned}\sigma^2 = \frac{1}{MN} + \left(\frac{1}{M}+\frac{1}{N}-\frac{2}{MN}\right)|\psi(\rho,\alpha)|^2 \\ -\left(\frac{1}{M}+\frac{1}{N}-\frac{1}{MN}\right)|\psi(\rho,\alpha)|^4. \end{aligned} \tag{7}$$

2) Every sensor as a transceiver: The localization metric in (2) can be rewritten as

$$A(\rho,\alpha) = \frac{1}{N^2}\left(\sum_{k=1,(k=l)}^{N} e^{j4\pi\rho u_k} + \sum_{k\neq l}^{N}\sum_{l=1}^{N} e^{j2\pi\rho(u_k+v_l)}\right) \tag{8}$$

Following steps similar to those in Section III-A1 above, we obtain

$$\phi(\rho,\alpha) = \frac{1}{N}\psi(2\rho,\alpha) + \frac{N-1}{N}\psi^2(\rho,\alpha) \tag{9}$$

and

$$\begin{aligned}\sigma^2 = \frac{2}{N^2} - \frac{1}{N^3} + 4\left(\frac{1}{N}-\frac{2}{N^2}+\frac{1}{N^3}\right)|\psi(\rho,\alpha)|^2 \\ -2\left(\frac{2}{N}-\frac{5}{N^2}+\frac{3}{N^3}\right)|\psi(\rho,\alpha)|^4 - \frac{1}{N^3}|\psi(2\rho,\alpha)|^2 \\ -2\left(\frac{1}{N^2}-\frac{1}{N^3}\right)\left(\psi(2\rho,\alpha)\psi^{*2}(\rho,\alpha)+\psi^*(2\rho,\alpha)\psi^2(\rho,\alpha)\right). \end{aligned} \tag{10}$$

For $\rho = 0$, the metric $A(0,\alpha) = 1$. It is easily verified that the variances $= 0$ at $\rho = 0$ in both (7) and (10). This is in agreement with the fact that the metric is assumed cohered at $\rho = 0$ irrespective of the sensors' locations.

3) Mean and variance for specific distributions of sensor locations: Here we make the localization metric A a function of a single variable by letting $\alpha = \pi/2$. This means that sidelobes are evaluated in the cross-range with respect to the sensors locations. We further assume two specific probability distributions for the sensor locations. In the first, u and v are assumed to be uniformly distributed in $[-u_{max}, u_{max}]$, where $u_{max} = \cos(\theta_{max} - \pi/2) = \sin\theta_{max}$. Computing the mean of $e^{j2\pi\rho u}$,

$$\psi(\rho) = \frac{\sin 2\pi\rho u_{max}}{2\pi\rho u_{max}}, \tag{11}$$

from which it follows that the mean localization pattern is given by

$$\phi(\rho) = \left(\frac{\sin 2\pi\rho u_{max}}{2\pi\rho u_{max}}\right)^2. \tag{12}$$

From (12), it is evident that the mean value of the localization pattern decays with ρ^2. It is also noted that the mean is independent of the number of sensors and is the same as that of a filled array between $-u_{\max}$ and $u_{\max}$. Fig. 2

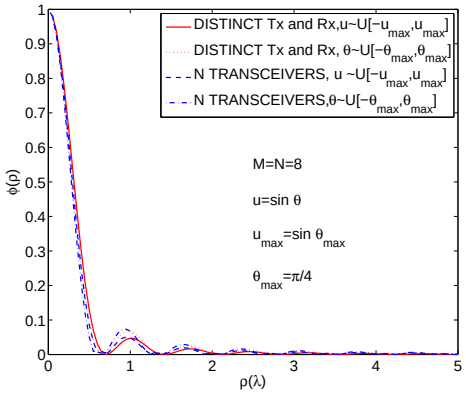

Fig. 2. Mean of the localization metric.

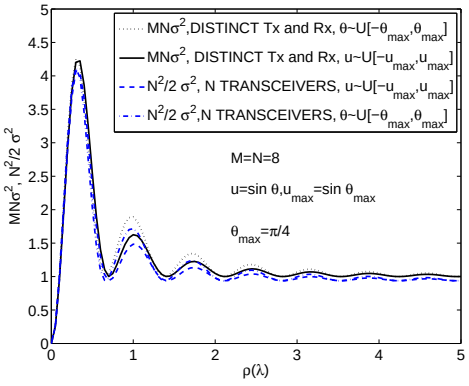

Fig. 3. Variance of the localization metric.

and 3 show the patterns of the means and variances for the two sensor distributions and for the two configurations, i.e.,

separate transmitters/receivers and transceivers. As seen in Fig. 2, the mean as a function of ρ from the coherence point is not significantly sensitive to the sensor configuration or the distribution of sensor locations. Shown in Fig. 3 are the plots of $MN\sigma^2$ versus ρ for separate transmitters/receivers configuration and $\frac{N^2}{2}\sigma^2$ versus ρ for all transceivers configuration. As observed from these plots and can be verified from (7) and (10), for distances larger than a few wavelengths, the variance in the case of distinct transmit and receive sensors approaches $1/MN$, whereas for the case with N sensors functioning as transceivers, the variance approaches $2/N^2$. Thus the variance for transceivers is twice as large as that with separate transmitters and receivers. This is in agreement with the fact that with M transmit sensors and $N = M$ receive sensors there are $MN = N^2$ distinct paths, whereas there are only $N + \binom{N}{2} = \frac{N^2}{2} + \frac{N}{2}$ distinct paths in the case of N transceivers. In the figures, the variances are given for $M = N = 8$ sensors. We conclude that in the sidelobes region, the variance of the localization metric decreases with the product of the number of sensors. MIMO radar will have an advantage over a single transmitter - multiple receivers architecture when $M + N << MN$.

B. Distribution of the peak sidelobe level

The distribution of the peak sidelobe level is a parameter of interest. The localization metric in (2) is a sum of iid complex random variables. By invoking the central limit theorem, the metric can be modeled with a Gaussian distribution. With the Gaussian assumption, the real and imaginary parts $A_1(\rho,\alpha)$ and $A_2(\rho,\alpha)$ of the metric are mutually independent. The joint probability density function (pdf) of A_1 and A_2 is the bivariate Gaussian pdf given by

$$f(A_1,A_2) = \frac{1}{2\pi\sigma_1\sigma_2}\exp\left\{-\frac{1}{2}\left[\frac{(A_1-\phi_1)^2}{\sigma_1^2}+\frac{(A_2-\phi_2)^2}{\sigma_2^2}\right]\right\}. \quad (13)$$

In (13) above, $\phi_1(\rho,\alpha)$ and $\phi_2(\rho,\alpha)$ are the means whereas σ_1^2 and σ_2^2 are the variances of respectively the real part A_1 and the imaginary part A_2 of the mean pattern $\phi(\rho,\alpha)$. The mean patterns for the separate transmitters/receivers configuration is given in (3) and for the transceivers configuration in (9). Closed form expressions for these variances have been derived by solving the equations resulting from the identities $E\left\{|A(\rho,\alpha)-\phi(\rho,\alpha)|^2\right\} = \sigma_1^2+\sigma_2^2$ and $\mathrm{Re}\left[E\left\{[A(\rho,\alpha)-\phi(\rho,\alpha)]^2\right\}\right] = \sigma_1^2-\sigma_2^2$, Re denoting the real part. The resulting expressions are omitted here for the sake of brevity. At any given location ρ, the probability that $|A(\rho)|$ is below a prescribed value q is given by

$$\Pr\{|A|<q\} = \int_{-q}^{q}\int_{-\sqrt{q^2-A_1}}^{\sqrt{q^2-A_1}} f(A_1,A_2)dA_1dA_2. \quad (14)$$

This probability distribution can be computed numerically. Fig. 4 illustrates the sidelobe patterns at different percentile values for the case of separate transmitters/receivers and $M = N = 8$. Since the variance in the case of N transceivers is twice that of $M = N$ separate transmitters/receivers, the sidelobe level outside of the mainlobe for the transceiver configuration would be $\sqrt{2}$ times as large as that of Fig. 4.

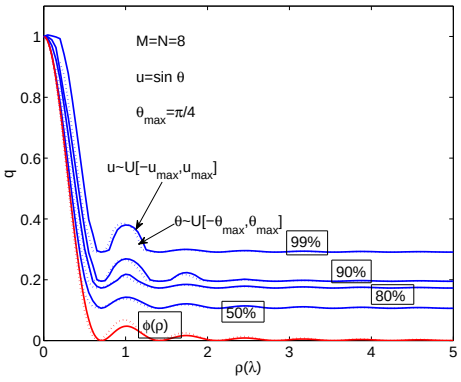

Fig. 4. Distribution of sidelobes with distinct transmit and receive sensors.

C. Confidence intervals and critical number of sensors

While statistics such as mean and variance provide important insight on the behavior of localization metric, a robust design requires the peak sidelobe levels of the localization metric to be bounded from above by a tolerable value. The requirements for a given sidelobe level and a confidence level are studied in this section.

We modeled $A(\rho,\alpha)$ in the sidelobe region using a Gaussian distribution as in (13). For large ρ, the means ϕ_1 and ϕ_2 approach zero. Accordingly the amplitudes $|A|$ have a Rayleigh distribution. It can be shown that for $\rho \gg 1$, the variances σ_1^2 and σ_2^2 approach $\sigma^2/2 \approx 1/2MN, 1/N^2$ respectively with separate transmitters/receivers and all sensors functioning as transceivers. Considering the former case, the cumulative probability of sidelobe level is given by

$$\Pr\{|A|<q\} = \int_0^q p(q)dq = 1-\exp\left(-MNq^2\right) \quad (15)$$

To determine the distribution of the peak sidelobe of the localization metric $|A(\rho)|$, we follow the reasoning in [5], where the problem is solved for a single transmitter. The statistics of $|A(\rho)|$ for all ρ of interest are determined by the statistics over a finite set of values ρ. This is due to the correlation between the values of $|A(\rho)|$ and $|A(\rho+\Delta\rho)|$, when $\Delta\rho$ is sufficiently small. To determine at how many points the statistics need to be determined, $\Delta\rho$ is evaluated from the autocorrelation function R_A of the localization pattern. We have

$$R_A(\rho,\nu) = E\left[(A(\rho)-\phi(\rho))(A(\nu)-\phi(\nu))^*\right].$$

After simple manipulations, we obtain for the case of separate transmitters/receivers

$$R_A(\rho,\nu) = \frac{1}{MN}\left[\phi(\rho-\nu)-\phi(\rho)\phi(\nu)\right].$$

To obtain a closed form solution, we use (12) for the case of uniform distribution of sensors in the u variable. For ρ, ν in the sidelobes, $\phi(\rho),\phi(\nu)\approx 0$, hence

$$R_A(\rho,\nu) \approx \left(\frac{\sin 2\pi\rho u_{max}}{2\pi\rho u_{max}}\right)^2.$$

We conclude that the width of the autocorrelation of the localization pattern is approximately $\Delta\rho \approx 1/2u_{\max}$. Let the surveillance area of interest be $|\rho| \leq \rho_{\max}$. It follows that the number of points at which the distribution of $|A(\rho)|$ has to be evaluated is $n = 2\rho_{\max}/(1/2u_{\max}) = 4\rho_{\max}u_{\max}$. Let β be the confidence level that none of the samples exceeds a given value q. Then β is related to the number of transmitters and receivers by

$$\begin{aligned} \beta &= Pr\{|A(\rho)| < q, \forall\rho, |\delta| < \rho \leq \rho_{\max}\} \\ &\approx \left[1 - \exp\left(-MNq^2\right)\right]^n. \end{aligned} \quad (16)$$

Here δ defines the region outside the mainbeam of the coherence point. In this region, the assumption that the mean pattern is negligible holds. The approximation is reached since $\delta \approx 1/2u_{\max}$. Thus using the Taylor series expansion of e^x we obtain

$$MN \approx \frac{1}{q^2}\left(\log n - \log\log\frac{1}{\beta}\right).$$

Fig. 5 shows the critical number of antennas plotted against the peak sidelobe level of the localization pattern $|A(\rho)|$ for separate transmitters receivers and sensors distributed uniform in u. It can be seen that for a peak sidelobe level of $0.3(= 20\log_{10} 0.3 \approx -10$ dB) with respect to the mainlobe, a confidence level of 95%, and a surveillance area with $\rho_{\max} = 100\lambda$, the critical number of sensors is $M = N \approx 10$ (a total of 20 sensors). It is not difficult to show that when all sensors are configured as transceivers, the above sidelobe level can be achieved with a total of only $10\sqrt{2} \approx 14$ sensors. In contrast, with the use of a single transmit antenna, the number of receiving sensors required to achieve the same performance is $MN = 100$. As seen from the curves, for different values of ρ_{max}, this critical number does not vary drastically even for substantial changes in the surveillance area.

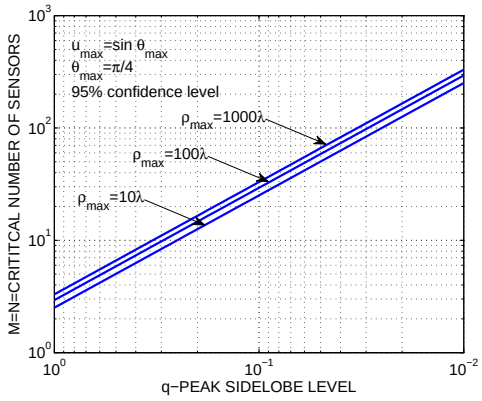

Fig. 5. Critical number of sensors as a function of the peak sidelobe level of the localization pattern $|A(\rho)|$.

IV. CONCLUSION

In the study presented in this paper, we developed a model of distributed coherent MIMO radar for active location estimation of targets in the near field. Under assumptions of the model, we were able to develop closed-form expressions for the mean and variance of the localization pattern and for the distribution of the peak sidelobes of the pattern. We obtained the following results on the mean of the localization pattern as a function of the distance from the coherence point of the MIMO radar array: (1) it is independent of the number of sensors; (2) it decays with the square of the distance from the coherence point; (3) it is the same as the pattern of a filled array extending between the extremal points of the MIMO sensors. The following results were shown on the variance of the localization pattern: (1) it vanishes in the neighborhood of the coherence point; (2) the variance of the sidelobes behaves as $1/MN$ for separate transmitters/receivers and as $2/N^2$ for transceivers, when the sensors are uniformly distributed between $-u_{\max} = -\sin\theta_{\max}$ and $u_{\max} = \sin\theta_{\max}$. Numerical results show that the variance is materially the same for the case when the uniform distribution of the sensors is in the bearing angle rather than in the sine of the bearing angle. Finally, a relation was developed between the critical number of sensors required to maintain peak sidelobe levels below a prescribed level and the desired confidence level of not exceeding the peak sidelobe level. For instance, it was found that $M = N = 10$ sensors are sufficient for limiting the sidelobe level to -10 dB with a 95% confidence level. It was found, the critical number of sensors is not sensitive to the size of the surveillance area.

The results obtained in this paper demonstrate that MIMO radar with M transmitters and N receivers perform as a radar system with 1 transmitter and MN receivers. Thus, the results underscore the gains for MIMO radar for cases when $M + N \ll MN$.

REFERENCES

[1] E. Fishler, A. Haimovich, R. Blum, L. Cimini, D. Chizhik, and R. Valenzuela, "Performance of MIMO radar systems: advantages of angular diversity," in *Proc. of 38th Asilomar Conf. on Signals, Systems and Computers,* Nov. 2004, pp. 305-309.

[2] E. Fishler, A. Haimovich, R. Blum, L. Cimini, D. Chizhik, and R. Valenzuela, "Spatial Diversity in Radars - Models and Detection Performance," *IEEE Trans. On Sig. Proc*., vol. 54, March 2006, pp.823-838.

[3] N.H. Lehmann, A.M Haimovich , R.S. Blum, L.J.Cimini, "High resolution capabilities of MIMO radar," in *Proc. of 40th Asilomar Conf. on Signals, Systems and Computers,* Nov. 2006.

[4] H. Godrich, A. M. Haimovich, and R. S. Blum "Target localization techniques and tools for MIMO radar" invited paper, *IEEE Radar Conference*, May 2008.

[5] Y. Lo, "A mathematical theory of antenna arrays with randomly spaced elements," *IEEE Transactions on Antennas and Propagation*, vol. 12, No. 3, pp. 257-268, May 1964.

[6] V. D. Agarwal, Y. T. Lo, "Distribution of Sidelobe Level in Random Arrays," Proc. IEEE, Oct. 1969, 1764-1765.

[7] B. D. Steinberg, "The peak sidelobe of the phased array having randomly located elements," *IEEE Trans. on Antennas and Propagation*, vol. AP-20, March 1972, pp. 129-136.

[8] B. D. Steinberg, "Radar Imaging from a Distorted Array: The Radio Camera Algorithm and Experiments," *IEEE Trans. on Antenna and Propagation*, Vol. AP-29, No. 5, pp. 740-748, Sep. 1981.

[9] A. Haimovich, R. Blum, and L. Cimini, "MIMO radar with widely separated antennas: Reviewing recent work," *IEEE Sig. Proc. Magazine*, January 2008, pp. 116-129.

[10] B. D. Steinberg, *Principles of Aperture and Array System Design*, John Wiley 1976.